Marine Biology (2001) 139: 497–506
DOI 10.1007/s002270100597

V. Kostylev · J. Erlandsson

A fractal approach for detecting spatial hierarchy and structure on mussel beds

Received: 14 December 2000 / Accepted: 4 April 2001 / Published online: 14 August 2001

Abstract Within beds of blue mussel (*Mytilus edulis* L.), individuals are aggregated into small patches, which in turn are incorporated into bigger patches, revealing a complex hierarchy of spatial structure. The present study was done to find the different scales of variation in the distribution of mussel biomass, and to describe the spatial heterogeneity on these scales. The three approaches compared for this purpose were fractal analysis, spatial autocorrelation and hierarchical (or nested) analysis of variances (ANOVA). The complexity (i.e. patchiness) of mussel aggregations was described with fractal dimension, calculated with the semivariogram method. Three intertidal mussel beds were studied on the west coast of Sweden. The distribution of wet biomass was studied along transects up to 128 m. The average biomasses of blue mussels on the three mussel beds were 1825 ± 210, 179 ± 21 and 576 ± 66 g per 0.1 m^2, respectively, and the fractal dimensions of the mussel distribution were 1.726 ± 0.010, 1.842 ± 0.014 and 1.939 ± 0.029 on transects 1–3, respectively. Distributions of mussels revealed multiscaling behaviour. The fractal dimension significantly changed twice on different scales on the first bed (thus showing three scaling regions), the second and third beds revealed two and three scaling regions, respectively. High fractal dimension was followed by significant spatial autocorrelation on smaller scales. The fractal analysis detects the multiple scaling regions of spatial variance even when the spatial structure may not be distinguished significantly by conventional statistical inference. The study shows that the fractal analysis, the spatial autocorrelation analysis and the hierarchical ANOVA give complementary information about the spatial variability in mussel populations.

Communicated by O. Kinne, Oldendorf/Luhe

V. Kostylev · J. Erlandsson (✉)
Tjärnö Marine Biological Laboratory,
45296 Strömstad, Sweden

Present addresses: V. Kostylev
Geological Survey of Canada,
Bedford Institute of Oceanography,
P.O. Box 1006, Dartmouth, Nova Scotia, Canada

Present address: J. Erlandsson
Coastal Research Group,
Department of Zoology and Entomology,
Rhodes University, Grahamstown 6140,
South Africa
e-mail: J.Erlandsson@ru.ac.za

Introduction

Estimation of scales of variation and the degrees of spatial heterogeneity is a necessary step to describe the distribution of natural populations, and for building a proper sampling design for later studies. Description of the variability and predictability of the environment requires reference to the particular range of scales that is relevant to the organisms or processes being examined (Levin 1992). In the present study we used three different approaches to address this problem: the commonly used techniques of spatial autocorrelation (Legendre and Fortin 1989) and hierarchical ANOVA (Underwood 1997), and the concept and tools of fractals, introduced by Mandelbrot (1977). A fractal is a complex geometrical shape, constructed of smaller copies of itself, and an ideal mathematical fractal has the same structure (is self-similar) on an infinite range of scales (Mandelbrot 1982). In contrast to simple geometric objects, fractals possess non-integer dimension. Geometric objects in Euclidean geometry are described using integer dimensions (0 for a point, 1 for a line, 2 for a plane and 3 for a volume), while fractal dimension does not need to be an integer. It may take any value between the bounding integer topological dimensions, and increases with the increase in complexity of a geometric object. For self-similar mathematical fractals, the fractal dimension (D) is calculated as:

$$D = \ln(N)/\ln(k) \quad (1)$$

for an irregular or fragmented geometric object that can be subdivided into N similar parts, each of which is a copy of the whole, reduced k times. Strict or ideal fractal shapes are not found in nature (although mathematical self-similarity may be visualised when viewing for example snowflakes and ferns down to a certain scale), which is why calculation of the fractal dimension of natural patterns and shapes is based on statistical self-similarity (classical examples are clouds and coastlines) and is done over a range of scales (see e.g. Cox and Wang 1993; Hastings and Sugihara 1993).

Fractal analyses describing the scaling of spatial and temporal patterns have been applied in some general ecological studies (e.g. Palmer 1988; Milne 1991; O'Neill et al. 1991). In marine pelagic ecology fractal and multifractal approaches have enhanced the knowledge of spatial heterogeneity in the distribution of phytoplankton and zooplankton (McClatchie et al. 1994; Pascual et al. 1995; Seuront and Lagadeuc 1997; Seuront et al. 1999), and in benthic ecology the estimation of fractal dimension has been used for the descriptions of gastropod movement patterns (Erlandsson and Kostylev 1995; Erlandsson et al. 1999), habitat complexity (e.g. Bradbury et al. 1984; Gee and Warwick 1994; Kostylev 1996; Kostylev et al. 1997; Erlandsson et al. 1999; Commito and Rusignuolo 2000) and spatial distribution of animals (Kostylev 1996; Snover and Commito 1998). It has been proposed that benthic communities in both marine and freshwater ecosystems show fractal properties (Azovsky et al. 2000; Schmid 2000).

All ecological systems exhibit heterogeneity and patchiness on a broad range of scales, and this patchiness is fundamental to population dynamics, and to many evolutionary and ecological processes (Levin 1992). The degree of aggregation in nature is always a function of spatial scale (Hurlbert 1990), and therefore an estimate of spatial variation on a continuous range of scales is important. The fractal concept allows consideration of both heterogeneity and scale together. Distribution patterns of hierarchically nested groupings can be self-similar for some scales of measurement and may possess another kind of partial self-similarity (different fractal dimensions) on others (Mandelbrot 1977). The existence of such multiple scaling regions is typical for many natural phenomena (Burrough 1981, 1983; Milne 1991; Hastings and Sugihara 1993; Seuront et al. 1999). Discontinuities between self-similar scaling parts may be indicative of changes in the natural scale of process-pattern relationships (Sugihara and May 1990), and should influence sampling design, information collection and system analysis.

The heterogeneity in the biomass distribution of marine animals arises as a result of their aggregated or patchy spatial occurrence. Spatial patchiness in the distribution of marine benthos may result from the action of both extrinsic and intrinsic, abiotic (e.g. hydrodynamics; Denny 1987) and biotic processes acting through dispersal and substratum selection, reproduction and recruitment variability, differential mortality and predation, competition for food and space, as well as different growth rates (Caley et al. 1996). Each of the influencing factors has a characteristic impact scale, and it is possible to assume the presence of several scaling regions evolving in the aggregation of benthic animals as a result of their influences. The blue mussel *Mytilus edulis* L. shows obvious clumped distribution at different spatial scales, mussels being aggregated into local patches, which in turn are incorporated into bigger patches, revealing a complex spatial structure. Mussel beds are important for benthic fauna by providing secondary space for bottom colonisation by many species, forming rough fractal substrates (Kostylev et al. 1997), and variation in the patchiness of mussels at hierarchical scales should therefore have consequences for variation in the associated benthic community structure. The present study examines the hypothesis of the existence of multiple scaling regions of variation in the distribution of blue mussels (*M. edulis*), and aims to compare and evaluate how informative and sensitive three different methods (fractal analyses, spatial autocorrelation and hierarchical ANOVA) are for detecting this kind of spatial hierarchy and structure in marine benthic populations.

Materials and methods

Study areas and sampling

Sampling was done in June 1992 (transect 1) and July 1995 (transects 2 and 3) on three beds of blue mussel (*Mytilus edulis*) around the island of Tjärnö, off the west coast of Sweden (Fig. 1), which is a coastline with very small tidal fluctuations (about 30–40 cm). Within the studied areas water depth varies between 0.1 and 1.5 m below chart datum. The first mussel bed is situated in the middle of a shallow strait with high water exchange. The bottom sediment consists of sand, gravel and mussel shells, which on the periphery is replaced by muddy sediments. Its central part is often exposed during low water levels. The second mussel bed is situated in a calm, closed bay with little water movements, on muddy sediment. The third mussel bed lies on a gently sloping side of a strait exposed to strong water currents, dominated by gravel and sandy substrata. Wet mussel biomass and density were estimated along transects sampled with a 0.1 m^2 quadrat frame at regular intervals of 2 m. A total of 64 quadrats were scraped and taken along each transect on the three mussel beds.

Data analysis

Fractal dimension

The semivariance ($Y_{(h)}$) was estimated as:

$$Y_{(h)} = 1/\left(2N_{(h)}\right) \sum_{x=1}^{N-h} \left(Z_{x+h} - Z_x\right)^2 \quad (2)$$

where N is the total number of data points, $N_{(h)}$ is the number of pairs of data points separated by the distance or lag h, Z_x and Z_{x+h} are the observed values of a regionalised variable at points x and $x+h$ (Burrough 1983).

Fractal dimension (D) was calculated as:

$$D = (4 - m)/2 \quad (3)$$

from the semivariogram (which is a log–log plot of $Y_{(h)}$ vs. h), where m is the absolute slope of the regression line (see e.g. Burrough 1983;

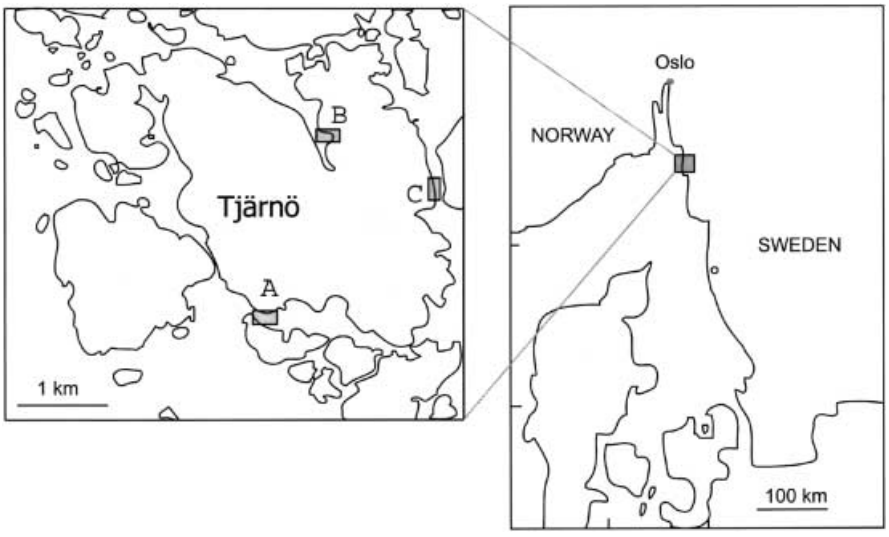

Fig. 1 The area studied. The transects, marked by *rectangles*, were sampled at sites A, B and C

Schmid 2000). The standard error of the fractal dimension was calculated as: SE(m)/2, which seems sensible from Eq. 3.

Estimating fractal dimension from a semivariogram is based on the properties of the fractional Brownian motion, which is a scale-invariant and self-similar process, generalised from the Brownian random function (Mandelbrot 1982). Hurst's exponent (H), which is a measure of persistence, equals 1/2 in ordinary random Brownian motion (Feder 1988). If $H > 1/2$ ($D < 1.5$) then the function expresses persistent behaviour. For example, if a positive increment exists from distance $-h$ to the observation point, then we will also have, on the average, an increase in the future (for the same distance). This case corresponds to spatial trends in data, e.g. to samples allocated along environmental gradients. For the case $H < 1/2$ ($D > 1.5$) an increasing trend in the past implies a decreasing trend in the future and vice versa, expressing antipersistent behaviour (Feder 1988). If we are considering the time series of a Brownian process (displacement vs. time) or a sequence of arbitrary values equally separated in space, then fractal dimension may be calculated from the relation:

$$D = 2 - H \tag{4}$$

Approximating spatial data with the fractional Brownian function allows the use of the semivariogram for estimating fractal dimension over a large range of scales, where variation of the dependent variable is considered a function of scale. Solving Eqs. 3 and 4 shows that Hurst's exponent equals half of the slope of a log–log semivariance plot.

The regression analysis of the semivariogram was made only for the scales less or equal to the half of the transect length, as semivariances for the larger scales do not represent variation between all data points. To distinguish partial regression lines with different slopes, the log–log regression line was fitted for the analysed half of the semivariogram, and residuals of the observed from the fitted values were calculated. In the presence of multiscaling, residuals regularly fluctuate around zero, forming periods of positive and negative deviations. For each such period (i.e. when residuals pertain the same sign), the maximal positive or negative value was assumed to correspond to a transition scale. The residual data were further divided into segments, lying between the transition scales. The simple linear regression was fitted for the residuals versus distance for each of the segments, and a statistically significant slope served as an indication that partial regression for the semivariogram on the distinguished interval must be used. For each of the intervals distinguished by the analysis of residuals, separate values of slopes for the log–log regression of semivariance versus spatial scale were calculated. Since this procedure includes multiple tests, the significance of individual slopes was estimated using the Bonferroni corrected level (Oden 1984; Legendre and Fortin 1989). The global test was made by checking whether the analysis contains at least one value which is significant at the $p' = p/k$ significance level (Legendre and Fortin 1989). The residual analysis was done recursively on each of the distinguished intervals until the partial regressions were significant. Slopes of distinguished piece-wise linear regressions were tested versus each other in order to eliminate possible redundancy. A similar method of residual analysis, but with other purposes, was used by Glejser (1969). Alternative approaches for the determination of transition points for partial regressions have been proposed by Nickerson et al. (1989) and Yeager and Ultsch (1989).

The slopes (m) of the piece-wise linear regressions were tested for significant deviation from Brownian expectations ($m = 1$; $D = 1.5$) and from very complex series ($m = 0$; $D = 2$) with one-tailed t-tests.

Fractograms (Palmer 1988) were built by plotting the fractal dimension versus scale. This method allows one to find out if spatial variation is generally self-similar and thus if one can make conclusions about variation at one scale based on another. The values of fractal dimension were calculated with Eq. 3 using 10-point sliding regression (estimating slopes of 1–10 pairs of data, 2–11, 3–12, etc.) of the semivariance versus scale.

Spatial autocorrelation

Spatial autocorrelation allows one to test statistically for the presence of spatial structure, obtaining significance of autocorrelation on each separate scale (Legendre and Fortin 1989). Spatial autocorrelation analysis was done using Geary's C coefficient:

$$C_{(h)} = (N-1)\sum_{x=1}^{N-h}(Z_{x+h} - Z_x)^2 / 2N_{(h)} \sum_{x=1}^{N}(Z_x - \bar{Z})^2 \tag{5}$$

where N is the total number of data points, $N_{(h)}$ is the number of pairs being compared, h is a lag, Zs are the observed values and $\bar{Z}$ is the average of the observed variable. These coefficients are computed for each distance class h. Computation was made using the R package (Legendre and Vaudor 1991). The correlogram was found significant if at least one $C_{(h)}$ value was significant at the Bonferroni-corrected P-level.

Hierarchical ANOVA

In contrast to semivariance, the hierarchical analysis of variance is a common method of testing a hypothesis statistically (Underwood

1997). The analysis was done according to the following model:

$$X_{ijklmn} = \mu + A_i + B(A)_{j(i)} + C[B(A)]_{k[j(i)]} + DC[B(A)]_{l\{k[j(i)]\}} + E(DC[B(A)])_{m(l\{k[j(i)]\})} + \epsilon_{ijklmn} \quad (6)$$

where X is abundance, A, B, C, D and E are effects of 64, 32, 16, 8 and 4 m scale, correspondingly, and ϵ_{ijklmn} is the error term. For this analysis the adjacent quadrats were grouped into pairs, thus forming replicates for the lowest considered level of variation (4 m), then pairs were grouped together and further on in the same fashion. As a result, variation on five spatial scales of doubling size was assessed.

Results

The three studied mussel beds had significantly different biomasses and densities. Figure 2 shows the biomass distributions along the transects. Average biomass of *Mytilus edulis* on the first, second and third bed was (mean ± SE) 1825 ± 210, 179 ± 21 and 576 ± 66 g per 0.1 m^2, respectively. Plot of the logarithm of semivariances versus spatial scales for all the studied mussel beds is presented in Fig. 3. The fractal dimension of the biomass variation on the first mussel bed, calculated for the range 2–64 m, was 1.726 ± 0.010. The results of partial regression analysis for transect 1 (Tables 1, 2, 3) allowed us to distinguish at least three scaling regions within this range. A very heterogeneous distribution on scales up to 16 m ($D = 1.800 \pm 0.024$) is followed by a much less heterogeneous distribution on scales up to 32 m ($D = 1.449 \pm 0.039$), which was not significantly different from random behaviour of the increment function. The biomass distribution becomes more heterogeneous again with significant antipersistent behaviour of increments on the scale up to 64 m ($D = 1.756 \pm 0.025$). The spatial autocorrelation shows the significant positive autocorrelation on the scale 2–18 m and negative on the scale 30–64 m (Table 4). Hierarchical ANOVA could not clearly distinguish differences in variation on different scales. However, there were indications that variation on scales 8 and 32 m is higher than on other scales ($P = 0.057$ and 0.062, respectively; the effect found significant on log-transformed data; Table 5).

The pattern of the semivariogram of transect 2 is generally similar to the first one (Fig. 3). The overall fractal dimension on the 2–64 m scale was 1.842 ± 0.014.

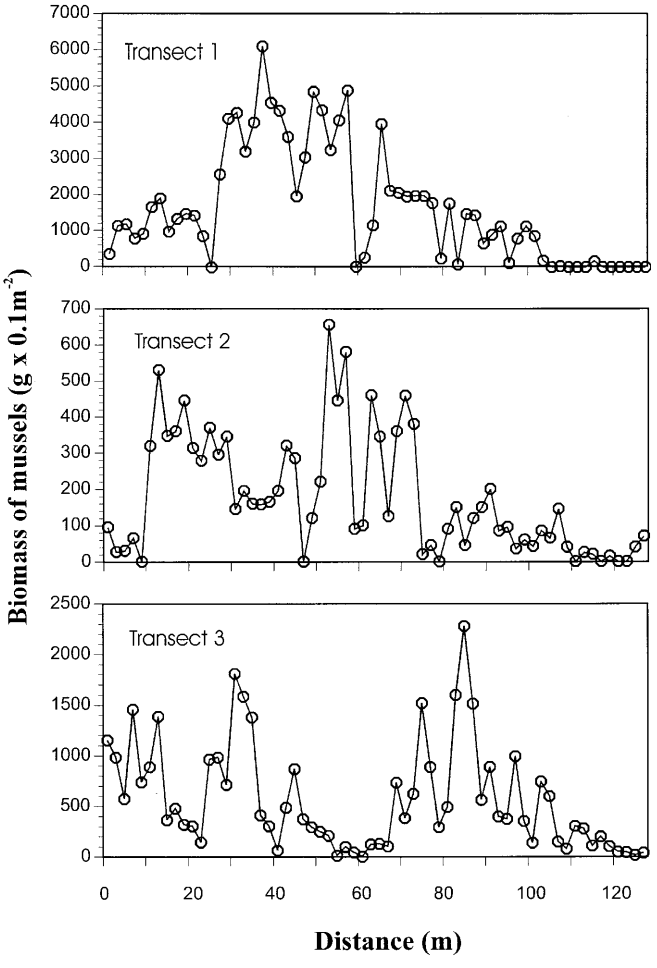

Fig. 2 *Mytilus edulis*. Distribution of biomass along the three transects

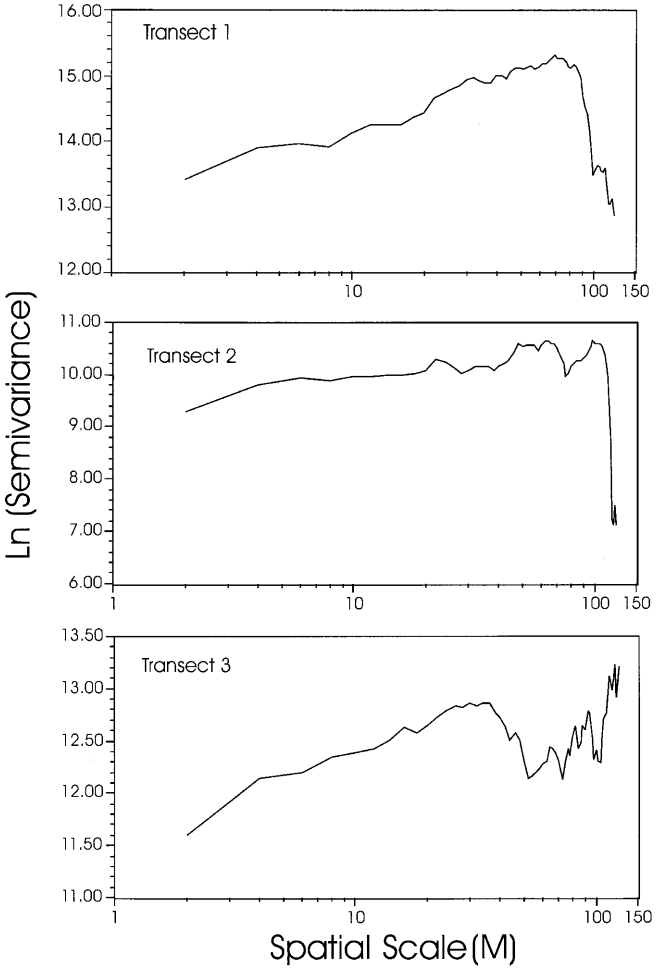

Fig. 3 Semivariogram. Plot of the logarithms of semivariance versus spatial scale (m) for the three studied mussel beds

Table 1 Regression coefficients and the fractal dimension (D) for the different spatial scales distinguished from the semivariograms

	Scale (m)	Slope	SE	t	P	D
Regressions						
Transect 1	2–64	0.551	0.020	27.91	0.0001	1.726
Transect 2	2–64	0.316	0.028	11.20	0.0001	1.842
Transect 3	2–64	0.122	0.058	2.084	0.0458	1.939
Partial regressions						
Transect 1	2–16	0.400	0.049	8.089	0.0001	1.800
	18–32	1.102	0.078	14.08	0.0001	1.449
	34–64	0.489	0.050	9.759	0.0001	1.756
Transect 2	2–38	0.230	0.032	7.284	0.0001	1.885
	40–64	0.892	0.178	5.009	0.0004	1.554
Transect 3	2–30	0.425	0.020	20.95	0.0001	1.788
	32–50	–1.158	0.149	–7.771	0.0001	1.421
	52–64	1.312	0.197	6.661	0.0012	1.344

Table 2 Comparison of regression slopes of the semivariogram for different distinguished scales of variation [$P(B)$ Bonferroni-corrected P-values]

Comparison	t	df	P	P(B)
Between transects				
Transect 1 vs. 2	6.829	126	0.0001	
Transect 1 vs. 3	6.993	126	0.0001	
Transect 2 vs. 3	3.012	126	0.005	
Within transects				
Transect 1: 2–16 vs. 18–32 m	7.621	12	0.001	0.003
Transect 1: 2–16 vs. 34–64 m	1.271	20	> 0.1	> 0.3
Transect 1: 18–32 vs. 34–64 m	6.616	20	0.001	0.003
Transect 2: 2–38 vs. 40–64 m	3.660	29	0.0001	0.0003
Transect 3: 2–30 vs 32–50 m	10.53	21	0.0001	0.0003
Transect 3: 2–30 vs. 52–64 m	4.479	20	0.0001	0.0003
Transect 3: 32–50 vs 52–64 m	9.999	13	0.0001	0.0003

A scale of high heterogeneity (2–38 m, $D = 1.885 \pm 0.016$) with significant antipersistent behaviour of increments is followed by the scale of lower heterogeneity (40–64 m, $D = 1.554 \pm 0.089$), where the variation of increments was not significantly different from random expectations ($t = 0.607$, $df = 11$; Table 3). The significant positive autocorrelation occurs on the scale of 2–8 m, followed by the negative autocorrelation on the scales 48–52 and 60–62 m (Table 4). Hierarchical analysis of variance did not find significant effects on any scale.

The variation of the mussel biomass along the third transect was different from the first two (Fig. 3). The overall fractal dimension on the 2–64 m scale was 1.939 ± 0.029. The fast growth of the semivariance on the scale 2–30 m ($D = 1.788 \pm 0.010$) is followed by a region of persistent behaviour of increments (32–50 m, $D = 1.421 \pm 0.074$) and then by the region of random variation in increments on the scale 52–64 m ($D = 1.344 \pm 0.098$; test for randomness: $t = 1.584$, $df = 5$, $P = 0.100$; Tables 1, 2, 3). The significant positive autocorrelation was observed on the scale 2–6 m, negative on 24–38 m and positive again on a 52–56 m scale (Table 4). Hierarchical ANOVA showed a significant effect on the 8 m scale (Table 5). Results from all analyses are presented in a comparative way in Fig. 4.

Thus, hierarchical analysis of variance shows that there is a significant difference in biomass of mussels separated by the distance 8 m at least in one case. Positive autocorrelation exists between biomasses generally on the scale < 18, 8 and 6 m (for the first, second and third transects, respectively). This allows one to assume the presence of a spatial structure of the size 6–18 m, within which biomass is similar. However, the scaling regions of the semivariance show that statistically the same relation between the variation of biomass and the spatial scale may hold for a much longer range (up to 38 and 30 m for the second and third transects, respectively).

The fractograms (Fig. 5) show the change in the locally estimated fractal dimension versus scale. On all of the three fractograms one can clearly observe

Table 3 Results of one-tailed t-tests for the comparison of the calculated slopes of the partial regressions of semivariance versus scale with the slope expected in case of random variation of increments ($m = 1$). Values in *bold* correspond to scales where the hypothesis of random variation of increments could not be disproved

	Scale (m)	t	df	P
Transect 1	2–16	12.24	6	0.0001
	18–32	1.308	6	**> 0.1**
	34–64	10.22	14	0.0001
Transect 2	2–38	–24.06	17	< 0.001
	40–64	0.607	11	**0.500**
Transect 3	2–30	–28.75	13	< 0.001
	32–50	–14.48	8	< 0.001
	52–64	1.584	5	**0.100**

Table 4 Geary's *C* coefficients for the scales 2–64 m. The *P*-values in *bold* indicate significant effects on the 0.05 significance level. The *C*-values <1 indicate positive autocorrelation, and those >1 negative autocorrelation

Distance (m)	Transect 1			Transect 2			Transect 3		
	C	Sign	*P*	*C*	Sign	*P*	*C*	Sign	*P*
2	0.276	+	**< 0.001**	0.452	+	**< 0.001**	0.395	+	**< 0.001**
4	0.460	+	**< 0.001**	0.688	+	**0.006**	0.678	+	**0.005**
6	0.493	+	**0.001**	0.772	+	**0.036**	0.715	+	**0.013**
8	0.468	+	**< 0.001**	0.743	+	**0.023**	0.820	+	0.082
10	0.584	+	**0.001**	0.795	+	0.059	0.855	+	0.135
12	0.659	+	**0.007**	0.807	+	0.074	0.889	+	0.203
14	0.668	+	**0.010**	0.809	+	0.080	0.977	+	0.434
16	0.665	+	**0.010**	0.821	+	0.096	1.104	–	0.194
18	0.744	+	**0.040**	0.829	+	0.111	1.051	–	0.318
20	0.787	+	0.076	0.831	+	0.116	1.113	–	0.184
22	0.997	+	0.492	1.058	–	0.304	1.211	–	0.059
24	1.062	–	0.300	0.993	+	0.481	1.294	–	**0.018**
26	1.145	–	0.146	0.929	+	0.314	1.344	–	**0.008**
28	1.201	–	0.081	0.849	+	0.156	1.337	–	**0.010**
30	1.332	–	**0.014**	0.896	+	0.247	1.388	–	**0.004**
32	1.383	–	**0.006**	0.937	+	0.340	1.354	–	**0.009**
34	1.303	–	**0.024**	0.939	+	0.347	1.393	–	**0.005**
36	1.254	–	**0.049**	0.891	+	0.244	1.381	–	**0.006**
38	1.273	–	**0.041**	0.846	+	0.167	1.263	–	**0.042**
40	1.413	–	**0.005**	0.928	+	0.328	1.214	–	0.079
42	1.409	–	**0.006**	1.023	–	0.406	1.102	–	0.237
44	1.331	–	**0.021**	1.016	–	0.422	0.979	+	0.450
46	1.483	–	**0.002**	1.221	–	0.077	1.032	+	0.387
48	1.583	–	**0.001**	1.452	–	**0.003**	0.974	+	0.440
50	1.536	–	**0.001**	1.356	–	**0.014**	0.799	+	0.119
52	1.459	–	**0.004**	1.416	–	**0.005**	0.675	+	**0.029**
54	1.517	–	**< 0.001**	1.234	–	0.072	0.684	+	**0.033**
56	1.582	–	**0.001**	1.182	–	0.124	0.713	+	**0.048**
58	1.518	–	**0.002**	1.107	–	0.238	0.738	+	0.065
60	1.448	–	**0.006**	1.359	–	**0.015**	0.770	+	0.092
62	1.431	–	**0.010**	1.334	–	**0.021**	0.798	+	0.121
64	1.489	–	**0.006**	1.255	–	0.058	0.909	+	0.299

Table 5 Hierarchical ANOVA of the biomass distribution of *Mytilus edulis* along the three transects (*S1* 64 m scale; *S2* 32 m scale; *S3* 16 m scale; *S4* 8 m scale; *S5* 4 m scale). Values in *bold* indicate significant effects on the *P*-level 0.05. Cochran's test for homogeneity of variances resulted in significant heterogeneity for the data of transect 1, but assumption of homogeneity was not disproved for transects 2 and 3. The *P*-values obtained for the analyses of the log-transformed data are indicated by *P**

Source	*df*	MS	*F*	*P*	*P**
Transect 1					
S1	1	4.228E7	2.170	0.279	0.356
S2(S1)	2	1.948E7	6.385	0.057	**0.034**
S3[S2(S1)]	4	3.051E6	0.994	0.464	0.451
S4{S3[S2(S1)]}	8	3.071E6	2.428	0.062	**0.005**
S5(S4{S3[S2(S1)]})	16	1.264E6	1.622	0.119	0.688
Residual	32	7.796E5			
Transect 2					
S1	1	3.602E5	5.564	0.142	0.263
S2(S1)	2	64,727.891	1.202	0.390	0.233
S3[S2(S1)]	4	53,836.141	1.907	0.203	0.114
S4{S3[S2(S1)]}	8	28,230.484	1.331	0.297	0.750
S5(S4{S3[S2(S1)]})	16	21,209.578	1.459	0.177	0.092
Residual	32	14,537.078			
Transect 3					
S1	1	1.213E5	0.065	0.823	0.871
S2(S1)	2	1.867E6	2.897	0.167	0.221
S3[S2(S1)]	4	6.443E5	1.226	0.372	0.082
S4{S3[S2(S1)]}	8	5.254E5	2.917	**0.033**	**0.044**
S5(S4{S3[S2(S1)]})	16	1.801E5	1.454	0.179	0.332
Residual	32	1.239E5			

depressions which correspond to the scales where distinct spatial structures are distinguished by partial regression. Fractograms as well as partial regressions allow the detection of three scaling regions in the distribution of blue mussels on the first mussel bed, two on the second and three on the third.

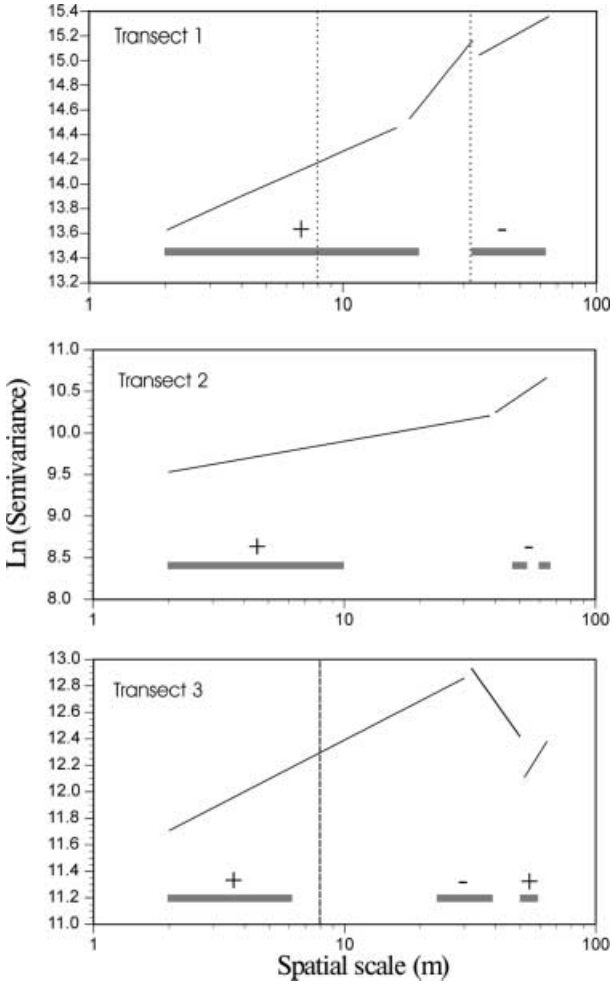

Fig. 4 Comparison of the spatial scales distinguished with the three different methods for mussel beds 1–3. Fitted intervals of the semivariance are shown with *solid lines*. *Shaded regions* correspond to the scales of the significant autocorrelation ($P < 0.05$; the sign of the correlation marked above the interval) found with Geary's C autocorrelation index. *Vertical dashed line* marks the scale of significant variation found with non-transformed data, and *dotted lines* indicate the scales of variation found for log-transformed data using nested analysis of variances

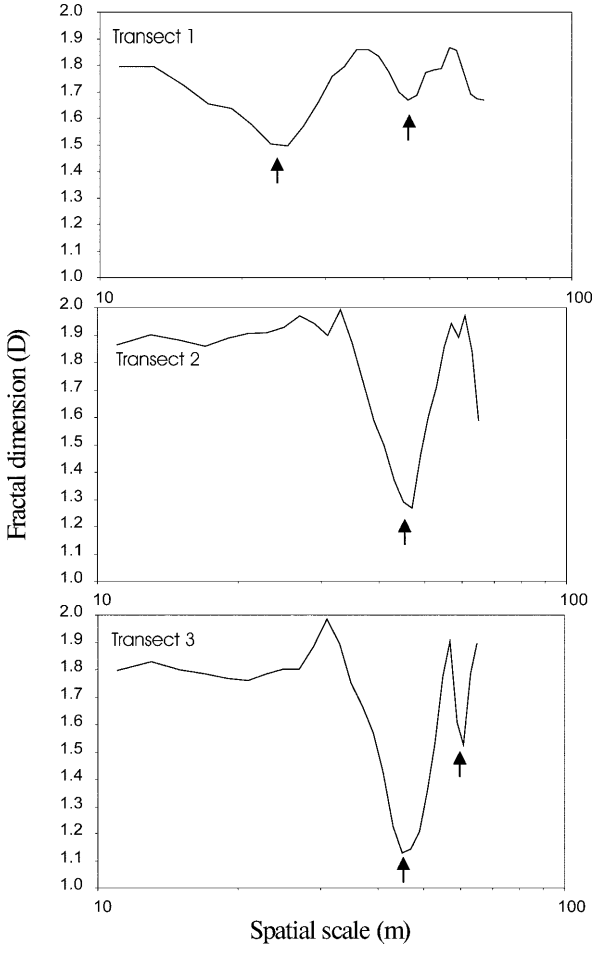

Fig. 5 Fractograms of biomass variation for the different transects, calculated from the semivariograms (see Fig. 3). The depressions marked with *arrows* correspond to the scales where the spatial structures found are most distinct

Discussion

The main reason for using fractals in the analysis of spatial patterns is that fractal dimension is an estimate of autocorrelation between *increments* of the spatial variable on different scales, and thus describes the spatial structure on specific scales. This means that if the correlation between increments on a certain scale is negative (antipersistence of increments), then an increasing trend is followed by a decreasing one and vice versa. The positive correlation of increments (persistence) implies that the trend has the same direction within the scales of reference. It is easy to see that antipersistence manifests presence of heterogeneity on the scale to which it applies, and persistent behaviour describes smooth spatial gradients or presence of a structure. It is possible to test statistically if the variation between increments is random, persistent or antipersistent.

Another valuable information obtained using the fractal approach is the detection of multiple scaling regions. The variation of increments of a spatial variable may be persistent on one scale, antipersistent or random on other scales, or be antipersistent on a global scale, while distributions may possess different levels of heterogeneity on local scales. Therefore, having distinguished different scaling regions of variation, one can assume the existence of hierarchical levels of heterogeneity or patchiness in the studied distribution. In a coral reef study (Bradbury et al. 1984), three scales of self-similarity were shown: on the scale of individual structure of coral colonies (~10 cm), in the distribution of sizes of living adult coral colonies (20–200 cm) and the spurs, grooves and other geomorphologic structures (5–10 m). Likewise, significantly different slopes of semivariance in the present study suggest the presence of different hierarchical scales of heterogeneity in the mussel beds.

Spatial autocorrelation and hierarchical ANOVA are often used by different schools of thought in spatial analysis (Legendre and Fortin 1989; Underwood 1997). All three approaches used in this study are different in how they test hypotheses and logical inference, which makes them complementary rather than redundant. We would like to emphasise that D and spatial autocorrelation express different properties of spatial structure. The fractal dimension calculated from the semivariance is a measure of rates in the change of variation versus scale. The rate of change in autocorrelation decreases with an increase in D (Rothrock and Thorndike 1980). The behaviour of the autocorrelation function is in fact identical to the behaviour of the semivariance function: the semivariance is a distance-type function and is related to Geary's C, with differences only in the denominator. On small spatial scales the high value of fractal dimension will manifest the presence of autocorrelation, and the slope of the log–log plot of the variance versus scale will lie close to 0 (Smith 1938). The increase in D is followed by the increase in the range of significant spatial autocorrelation on the smaller scales, indicated as grey bars in Fig. 4. Thus, when spatial autocorrelation analysis is used in separate tests of the significance of the correlation coefficient being different from zero, on each scale separately, the fractal scaling analyses the rate of change in autocorrelations. Additionally, a significant correlation coefficient on one scale implies that values of analysed variables are rather close to each other, without giving information about the direction of variation.

The mussel bed (*Mytilus edulis*) data show that positive autocorrelation at short distances is coupled with negative autocorrelation for long distances, which are typical results for the analysis of environmental data (Legendre and Fortin 1989), and which were observed for transects 1 and 2. Such results may be obtained for spatial gradients with contagious distribution at short distances. The fractal analysis shows that these differences arise from the existence of several levels of patchiness. In the case of transect 1, small-scale patchiness (2–16 m) is replaced by the presence of random fluctuation of increments (18–32 m), which then evolve into a large spatial structure that represents the whole mussel bed (34–64 m). On the second mussel bed, patchy distribution of biomass on the smaller scale is superimposed on random variation of increments on the 40–64 m scale. In the case of the third transect, positive correlation on small scales is replaced by negative on larger scales, and then again by positive autocorrelation on an even larger scale, which exposes the presence of large, repeated structures. This result is clearly seen from the partial regression analysis which distinguishes patchiness on the 2–30 m scale, a spatial trend on the 32–50 m scale and random variation of increments on the 52–64 m scale.

Hierarchical ANOVA has been shown to be a powerful tool in marine ecology (Underwood 1997), and has been applied to the analysis of spatial patterns in marine benthos (e.g. Morrisey et al. 1992; Lindegarth et al. 1995; Lawrie and McQuaid 2001). This approach is undoubtedly to be preferred in studies of large-scale distributions, where the logistics would not allow continuous sampling. Hierarchical ANOVA allows one to find out if a certain spatial scale introduces a significant variation in the data. So, in contrast to the fractal analysis, which looks for scaling regions and rates of change in spatial variation, and similarly to the spatial autocorrelation analysis, ANOVA looks for a patch size. Hierarchical ANOVA tests for the presence of spatial structure by the significance of increase in the mean square on a scale of interest compared to the scale below (ratio between the mean square of the upper level vs. the mean square of the next lower level). The plot of the variance estimated as the mean square calculated for each nested spatial level is shown in Fig. 6. The changes

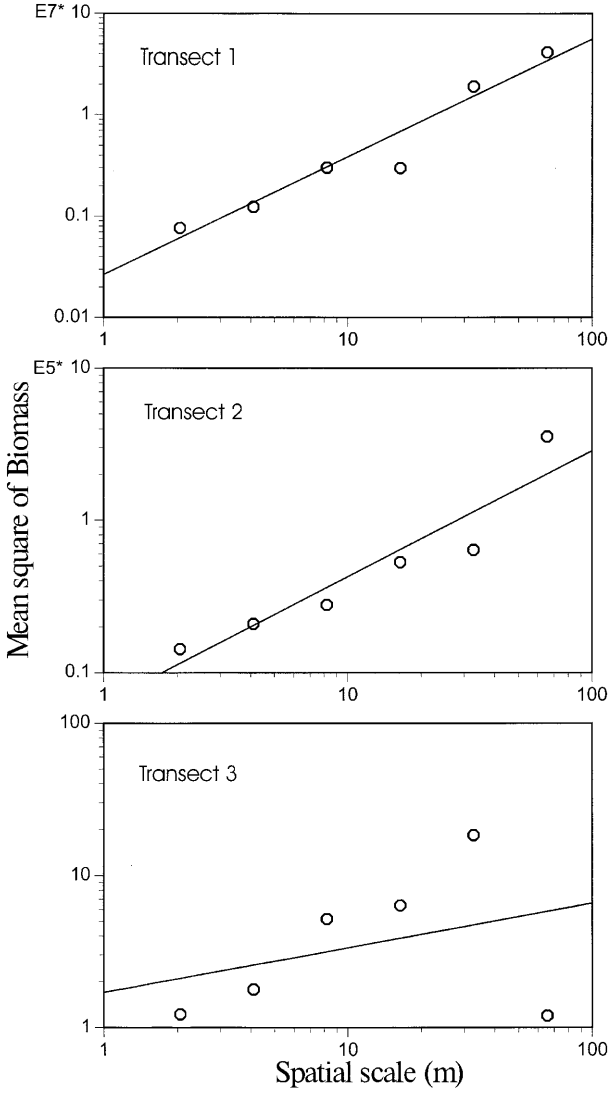

Fig. 6 Mean square of biomass versus the spatial scale on the three mussel beds (see legend of Table 5 for details). The regression may allow calculation of the fractal dimension in the same way as for the semivariance plot (see "Discussion")

in the mean square in relation to the scale closely follow changes in the semivariance (Figs. 3, 4). It appears possible (although this needs to be proved algebraically) that one can also calculate the fractal dimension of the biomass distribution from the mean square plot, analogous to the calculation from a semivariogram. This is probably true when assumptions underlying semivariance analysis (data are stationary) and ANOVA (homogeneity of variances and independence of samples) are satisfied and spatial structure is present. However, D calculated from the mean squares plot and from the semivariogram may not be directly comparable, as they are calculated from regressions based on different numbers of examined scales. Moreover, the semivariance accounts for variation in the individual data values, while hierarchical ANOVA accounts for variation in averages of spatially grouped values. Due to the effect of grouping the hierarchical design may miss the changes in variation on intermediate scales that makes it difficult to find the transition zones between different scaling regions.

The results of all three approaches of spatial analysis give different aspects of knowledge about mussel distributions. Autocorrelation analyses succeeded to pick up the major general structure. The fractal analysis showed that the spatial variation within beds has several scaling regions due to the nesting of patchiness on different scales. Within scaling regions the spatial variance changes monotonically. This, in consequence, did not allow ANOVA to distinguish a clear spatial structure on non-transformed data in two cases out of three.

The spatial variation on larger scales on mussel beds may be explained by variation in the characteristics of sediments (which are often heterogeneous, Burrough 1981, 1983), turbulent transport, and disturbances such as hydrodynamic forces (Denny 1987) affecting mussel settlement, food supply and adult mussels. On smaller scales, the variation in mussel biomass may be caused mainly by intraspecific competition, selective predation (for example, by crabs) and recruitment variability (Caley et al. 1996).

The present study has demonstrated how fractal analysis may be used to describe spatial heterogeneity of biomass in natural populations of mussels. It is possible to extend this analysis to other variables on a mussel bed (such as packing complexity, surface roughness and size-frequency distribution). Snover and Commito (1998) used the box-counting method (e.g. Hastings and Sugihara 1993) to estimate the fractal dimension of the outline of the spatial pattern created by aggregations of *M. edulis*, suggesting that the complexity of patch borders could be another variable for describing mussel distributions. There may, however, be some methodological problems involved with the box-counting method (see Erlandsson and Kostylev 1995) and with the estimations of patch geometry and spatial aggregation on a horizontal plane in given quadrats and subquadrats. These different types of complexities may have different ecological significances for mussels and co-existing fauna. A full description of the complex spatial patterns characteristic of natural populations should serve as a valuable part in the formulation of relevant hypotheses and experimental tests.

Acknowledgements We are grateful to R. Kostyleva for the help in collecting and processing samples, to Prof. P. Legendre for the use of his computer package on spatial statistics, and to Prof. D. Borcard for useful comments and suggestions. We also thank Prof. P. Jonsson, Dr. M. Villet and three anonymous reviewers for helpful comments on earlier drafts of the manuscript. This study was funded by a grant from the Central European University (Soros Foundation) to V.K. The study complies with the Swedish laws.

References

Azovsky AI, Chertoprood MV, Kucheruk NV, Rybnikov PV, Sapozhnikov FV (2000) Fractal properties of spatial distribution of intertidal benthic communities. Mar Biol 136:581–590

Bradbury RH, Reichelt RE, Green DG (1984) Fractals in ecology: methods and interpretation. Mar Ecol Prog Ser 14:295–296

Burrough PA (1981) Fractal dimensions of landscapes and other environmental data. Nature 294:240–242

Burrough PA (1983) Multiscale sources of spatial variation in soil. 1. The application of fractal concepts to nested levels of soil variation. J Soil Sci 34:577–597

Caley MJ, Carr MH, Hixon MA, Hughes TP, Jones GP, Menge BA (1996) Recruitment and the local dynamics of open marine populations. Annu Rev Ecol Syst 27:477–500

Commito JA, Rusignuolo BR (2000) Structural complexity in mussel beds: the fractal geometry of surface topography. J Exp Mar Biol Ecol 255:133–152

Cox BL, Wang JSY (1993) Fractal surfaces: measurement and application in the earth sciences. Fractals 1:87–115

Denny MW (1987) Lift as a mechanism of patch initiation in mussel beds. J Exp Mar Biol Ecol 113:231–245

Erlandsson J, Kostylev V (1995) Trail following, speed and fractal dimension of movement in a marine prosobranch, *Littorina littorea*, during a mating and a non-mating season. Mar Biol 122:87–94

Erlandsson J, Kostylev V, Williams GA (1999) A field technique for estimating the influence of surface complexity on movement tortuosity in the tropical limpet *Cellana grata* Gould. Ophelia 50:215–224

Feder J (1988) Fractals. Plenum, New York

Gee JM, Warwick RM (1994) Metazoan community structure in relation to the fractal dimensions of marine macroalgae. Mar Ecol Prog Ser 103:141–150

Glejser H (1969) A new test for heteroscedascity. J Am Statist Assoc 64:316–323

Hastings HM, Sugihara G (1993) Fractals: a user's guide for the natural sciences. Oxford University Press, New York

Hurlbert SH (1990) Spatial distribution of the montane unicorn. Oikos 58:257–271

Kostylev V (1996) Spatial heterogeneity and habitat complexity affecting marine littoral fauna. PhD thesis, Göteborg University, Göteborg, Sweden

Kostylev V, Erlandsson J, Johannesson K (1997) Microdistribution of the polymorphic snail *Littorina saxatilis* (Olivi) in a patchy rocky shore habitat. Ophelia 47:1–12

Lawrie SM, McQuaid CD (2001) Scales of mussel bed complexity: structure, associated biota and recruitment. J Exp Mar Biol Ecol 257:135–161

Legendre P, Fortin MJ (1989) Spatial pattern and ecological analysis. Vegetatio 80:107–138

Legendre P, Vaudor A (1991) The R package: multidimensional analysis, spatial analysis. Department of Biological Sciences, University of Montreal, Montreal

Levin SA (1992) The problem of pattern and scale in ecology. Ecology 73:1943–1967
Lindegarth M, Andre' C, Jonsson PR (1995) Analysis of the spatial variability in abundance and age structure of two infaunal bivalves, *Cerastoderma edule* and *C. lamarcki*, using hierarchical sampling programs. Mar Ecol Prog Ser 116:85–97
Mandelbrot BB (1977) Fractals: form, chance and dimension. Freeman, San Francisco
Mandelbrot BB (1982) The fractal geometry of nature. Freeman, New York
McClatchie S, Greene CH, Macaulay MC, Sturley DRM (1994) Spatial and temporal variability of Antarctic krill: implications for stock assessment. ICES J Mar Sci 51:11–18
Milne BT (1991) Heterogeneity as a multiscale characteristic of landscapes. In: Kolasa J, Pickett STA (eds) Ecological heterogeneity. Springer, New York Berlin Heidelberg , pp 69–84
Morrisey DJ, Howitt L, Underwood AJ, Stark JS (1992) Spatial variation in soft-sediment benthos. Mar Ecol Prog Ser 81:197–204
Nickerson DM, Facey DE, Grossman GD (1989) Estimating physiological thresholds with continuous two-phase regression. Physiol Zool 62:866–887
Oden NL (1984) Assessing the significance of a spatial correlogram. Geographical Anal 16:1–16
O'Neill RV, Gardner RH, Milne BT, Turner MG, Jackson B (1991) Heterogeneity and spatial hierarchies. In: Kolasa J, Pickett STA (eds) Ecological heterogeneity. Springer, New York Berlin Heidelberg, pp 85–96
Palmer MW (1988) Fractal geometry: a tool for describing spatial patterns of plant communities. Vegetatio 75:91–102
Pascual M, Ascioti A, Caswell H (1995) Intermittency in the plankton: a multifractal analysis of zooplankton biomass variability. J Plankton Res 17:1209–1232
Rothrock DA, Thorndike AS (1980) Geometric properties of the underside of sea ice. J Geophys Res 85:3955–3963
Schmid PE (2000) Fractal properties of habitat and patch structure in benthic ecosystems. Adv Ecol Res 30:339–401
Seuront L, Lagadeuc Y (1997) Characterisation of space-time variability in stratified and mixed coastal waters (Baie des Chaleurs, Quebec, Canada): application of fractal theory. Mar Ecol Prog Ser 159:81–95
Seuront L, Schmitt F, Lagadeuc Y, Schertzer D, Lovejoy S (1999) Universal multifractal analysis as a tool to characterize multiscale intermittent patterns: example of phytoplankton distribution in turbulent coastal waters. J Plankton Res 21:877–922
Smith HF (1938) An empirical law describing heterogeneity in the yields of agricultural crops. J Agric Sci 28:1–3
Snover ML, Commito JA (1998) The fractal geometry of *Mytilus edulis* L. spatial distribution in a soft-bottom system. J Exp Mar Biol Ecol 223:53–64
Sugihara G, May RM (1990) Applications of fractals in ecology. Trends Ecol Evol 5:79–86
Underwood AJ (1997) Experiments in ecology: their logical design and interpretation using analysis of variance. Cambridge University Press, Cambridge
Yeager DP, Ultsch GR (1989) Physiological regulation and conformation: a BASIC program for the determination of critical points. Physiol Zool 62:888–907